ELSEVIER

Contents lists available at ScienceDirect

Deep-Sea Research Part II

journal homepage: www.elsevier.com/locate/dsr2





Parameterization of ocean surface wave-induced mixing using Large Eddy Simulations (LES) II

Haili Wang a,b,c , Changming Dong d,e,f,* , Baylor Fox-Kemper g,** , Qing Li h , Yongzeng Yang i,j,k , Xu Chen l , Kenny T.C. Lim Kam Sian d,m

- a State Key Laboratory of Tropical Oceanography, South China Sea Institute of Oceanology, Chinese Academy of Sciences, Guangzhou, China
- ^b Southern Marine Science and Engineering Guangdong Laboratory (Guangzhou), Guangzhou, China
- ^c Innovation Academy of South China Sea Ecology and Environmental Engineering, Chinese Academy of Sciences, Guangzhou, China
- ^d School of Marine Sciences, Nanjing University of Information Science & Technology, Nanjing, China
- e Southern Marine Science and Engineering Guangdong Laboratory (Zhuhai), Zhuhai, China
- f Institute of Geophysics and Planetary Physics, University of California, Los Angeles, CA, USA
- g Department of Earth, Environmental and Planetary Sciences, Brown University, Providence, RI, USA
- h Thrust of Earth, Ocean and Atmospheric Sciences, The Hong Kong University of Science and Technology (Guangzhou), Guangzhou, China
- i First Institute of Oceanography, Ministry of Natural Resources, Qingdao, China
- ^j Laboratory for Regional Oceanography and Numerical Modeling, Qingdao National Laboratory for Marine Science and Technology, Qingdao, China
- ^k Key Laboratory of Marine Science and Numerical Modeling, Ministry of Natural Resources, Qingdao, China
- ¹ College of Physical and Environmental Oceanography, Ocean University of China, Qingdao, China
- ^m College of International Education, Wuxi University, Wuxi, China

ARTICLE INFO

Keywords: Wave-induced mixing Turbulence parameterization GOTM Large eddy simulation

ABSTRACT

The ocean surface boundary layer links the atmosphere to the ocean. At the air-sea interface, ocean surface waves play an important role in momentum, energy and gas exchange. A new parameterization with wave-induced mixing is developed based on a set of Large Eddy Simulation experiments under different wind speeds and mixed layer depths. The new parameterization scheme is then incorporated into a one-dimensional turbulence model for verification. The inclusion of wave-induced mixing reduces the excessively high surface temperature simulated in summer and reduces the underestimation of the mixed layer depth in winter. Compared to the observation at Ocean Station Papa, the parameterization scheme with wave effects produces statistically more accurate results than the parameterization scheme without wave effects.

1. Introduction

The ocean surface boundary layer (OSBL) is an integral part of the climate system, controlling the heat and momentum transport between the atmosphere and ocean. The flow within the OSBL, affected strongly by wind, wave and buoyancy fluxes, is mostly turbulent. Wind blowing over the ocean produces surface gravity waves, which interact with background turbulence previously present in the OSBL (Teixeira and Belcher, 2002), and thus play an essential role in air-sea momentum exchange and upper ocean mixing. Compared with other physical processes such as ocean currents, tides and internal waves, surface wave motions have a smaller spatial and temporal scale (Webb and Fox-Kemper, 2011, 2015). However, because waves are persistent and

common in space and time, they can affect large-scale phenomena. Many studies point out that including the effects of wind-driven waves is important in reducing the mismatch between climate simulations and observations (Sullivan and McWilliams, 2010; Belcher et al., 2012; Cavaleri et al., 2012; D'Asaro et al., 2014; Qiao et al., 2013; Li et al., 2016).

However, the effect of waves on vertical mixing is not considered in many OSBL turbulent mixing parametrization schemes. Wave-induced mixing is crucial to vertical mixing (Li et al., 2019). Vertical turbulent mixing influences the mixed layer depth (MLD) and thereby the heat capacity of the layer in immediate contact with the atmosphere (Balaguru et al., 2015). Small sea surface temperature (SST) deviations may significantly influence atmospheric convection. The mixed layer largely

E-mail addresses: cmdong@nuist.edu.cn (C. Dong), baylor@brown.edu (B. Fox-Kemper).

^{*} Corresponding author. School of Marine Sciences, Nanjing University of Information Science & Technology, Nanjing, China.

^{**} Corresponding author.

coincides with the euphotic zone and is critical for marine primary productivity in biological models. The effect of turbulent mixing in the OSBL, and the related feedback to the atmosphere, is not correct when wave effects are not considered.

Over the past few decades, as our understanding of wave-induced mixing increased, more studies focusing on the parameterization of wave-induced mixing effects have been conducted. Qiao et al. (2004) propose a non-breaking wave-induced mixing parameterization scheme, which is similar to the scheme to be introduced in Section 3, in that it generates more mixing when waves are strong. However, it differs in its theoretical basis from the scheme under study here, which is derived from the wave-averaged equations (Craik and Leibovich, 1976) and represents the effect of Langmuir turbulence (McWilliams et al., 1997). Averaging over a wave period following the trajectories of fluid parcels gives a net flow in the direction of wave propagation, known as the Stokes drift (van den Bremer and Breivik, 2018; Webb and Fox-Kemper, 2011, 2015). The Stokes drift and surface flow interact to drive the Langmuir circulation (LC) and its disordered variant, the Langmuir turbulence (LT), in the wave-averaged equation formulation (Craik and Leibovich, 1976; Lane et al., 2007; McWilliams et al., 2004; Suzuki and Fox-Kemper, 2016), which is important for vertical mixing (Li et al., 2019). LT has been considered by many researchers in the study of wave-induced mixing parameterization (e.g. Ali et al., 2019; McWilliams and Sullivan, 2000; Noh et al., 2016; Smyth et al., 2002; Van Roekel et al., 2012). The effect of Langmuir mixing can be accounted for by an amplification factor to the eddy viscosity and diffusivity in simple first-order turbulence closure schemes (e.g. McWilliams and Sullivan, 2000), and by additional Stokes drift related terms such as the turbulent kinetic energy production and pressure correlation in second-order closure schemes (Harcourt, 2013, 2015; Kantha and Clayson, 2004). The improved parameterizations with wave-induced mixing have been applied to ocean and climate models (Li et al., 2016; Li and Fox-Kemper, 2017; Noh et al., 2016). The introduction of the amplification factor into the K-profile parameterization (KPP) formulation proposed by McWilliams and Sullivan (2000) overestimates the effect of Langmuir circulation under strong convection (Fan and Griffies, 2014; Li et al., 2016; Smyth et al., 2002), and an improved version is proposed by Li et al. (2016). Moreover, the effect of breaking waves (BW) is not taken into account in previous LT studies.

In Wang et al. (2020), the sensitivity of turbulence to monochromatic and wind-induced polychromatic waves in wave-averaged Large Eddy Simulation (LES) experiments is analyzed with the influence of BW. The results show that the Stokes drift calculated from wind (polychromatic waves) is significantly different (and more accurate) from monochromatic waves-estimated Stokes drift (see also Kukulka and Harcourt, 2017). Therefore, the effect of polychromatic waves is essential to represent the real sea state (see also Webb and Fox-Kemper, 2015, 2011). In this study, a Stokes drift profile corresponding to fully-developed, unidirectional waves as a function of wind speed is used to investigate LT and LT-induced mixing with the influence of BW. The rest of the study is as follows: The second section describes the experimental setting, the third section is the parameterization study, the fourth section is the application of the parameterization scheme, and the last section is the summary and discussion.

2. Method and experiment configuration

2.1. LES experiment configuration

In this study, we use the LES model to resolve LT and parameterize BW. In LES models, scales larger than the filter width are directly simulated, while scales smaller than the filter width are parameterized by a turbulence closure model. The Parallelized Large-Eddy Simulation Model (PALM; Maronga et al., 2015) is applied in this study to investigate the effects of LC and BW. The filtered equation is as follows:

$$\frac{\partial u_i}{\partial t} + \left(u_j + u_{sj}\right) \frac{\partial u_i}{\partial x_i} = -\frac{1}{\rho_o} \frac{\partial p}{\partial x_i} - \varepsilon_{ijk} f_j(u_k + u_{sk}) + \varepsilon_{ijk} u_{sj} \omega_k - \frac{\partial \tau_{ij}}{\partial x_i} + F_i$$
 (1)

$$F_{i} = \frac{\alpha u^{*}}{t_{0}} G(0; 1) (1 - \delta_{i3}) \delta(z)$$
 (2)

where u_i is the Eulerian current velocity, subscripts i, j, k $\in \{1,2,3\}$ indicate vector components, u_{sj} is the Stokes velocity, x_i is the location coordinate, and ρ_o is the ocean density, p is dynamic pressure (modified from the thermodynamic pressure to account for waves; Suzuki and Fox-Kemper, 2016), ε is the Levi-Civita symbol, f is the Coriolis parameter, ω is the vorticity or curl of the Eulerian velocity, and τ_{ij} is the subgrid-scale Reynolds stress. F_i represents the random forcing (i.e. BW-induced small-scale turbulence assuming that the random forcing exists only at the sea surface; Noh et al., 2016), u^* is the frictional velocity, G(0;1) is the Gaussian distribution, δ is the Kronecker delta, $t_0=0.125/\alpha u^*$ is the time scale and $\alpha=3$ is a proportionality constant (Noh et al., 2004). For simplicity, both the wind stress and wave fields are assumed to be in the x-direction.

The model domain is $300 \times 300 \times 60$ grid points, with a 1.25 m grid resolution in the horizontal and vertical directions. Surface cooling is applied at the beginning of the simulation for 900 s to initiate turbulent motions, the detailed information can be found in Noh et al. (2004). The domain is doubly-periodic in the horizontal and a free-slip bottom boundary condition is used. The Stokes velocity required in Equation (1) can be simply parameterized following Equation (3) below (Kenyon, 1969; McWilliams and Restrepo, 1999) if the fully-developed, unidirectional Pierson and Moskowitz (1964) wave spectrum form is assumed:

$$u_{sj} = 0.04U \exp\left[-\frac{4\sqrt{g|z|}}{W}\right] \tag{3}$$

where g is the gravitational acceleration, U is the wind speed 10 m above the sea surface (a vector quantity) and W = |U| is the absolute wind speed (a scalar). We note that more accurate Stokes drift profiles based on empirical wave spectra, including wave age and directional spreading, are also known (Webb and Fox-Kemper, 2011, 2015). These profiles tend to have stronger surface Stokes drift for the same depth-integrated Stokes drift and thus larger Stokes shear, which tends to drive stronger LT (Suzuki and Fox-Kemper, 2016). Therefore, the use of profiles is a conservative lower estimate of the mixing strength by LT.

A series of numerical experiments (Table 1) are conducted to examine the effects of LC and BW on the upper mixed layer. The wind stress equation $\tau = \rho_a C_D U^2 = \rho_0 u^{*2}$ (where C_D is the drag coefficient and ρ_a is the air density) has been applied in which C_D is calculated following Large and Pond (1982).

$$C_D \times 10^3 = \begin{cases} 1.14 & 3 < U < 10ms^{-1} \\ 0.49 + 0.065 \times U & 10 < U < 25 \, ms^{-1} \end{cases}$$
 (4)

In Table 1, a new parameter (La_{SL}) is introduced. La_{SL} is the surface average Langmuir turbulence number, $La_{SL} = \sqrt{u^*/(u_{SL}^s - u_{ref}^s)}$, $u_{SL}^s = \sqrt{u^*/(u_{SL}^s - u_{ref}^s)}$, $u_{SL}^s = \sqrt{u^*/(u_{SL}^s - u_{ref}^s)}$

$$\left|\left(\int\limits_{-H_{SL}}^{0}u^{S}(z)dz\right)/H_{SL}\right|$$
 , where $H_{SL}=0.2h_{b},\,h_{b}$ is the boundary layer depth,

and u_{ref}^s is the Stokes drift velocity at the reference depth, which is usually thought as the bottom value. The subscript *ref* represents the reference quantity, and the superscript *s* denotes the Stokes drift (Harcourt and D'Asaro, 2008).

2.2. GOTM experiment configuration

To apply the parameterization under realistic forcing purposes, the study employs the fifth edition of the General Ocean Turbulence Model (GOTM5; https://gotm.net/; Umlauf and Burchard, 2005). Our method

Table 1 List of numerical experiments with different combinations of wind speed (U, m/s), initial MLD (m), surface friction velocity (u*, m/s) and surface average Langmuir turbulence number (La_{sL}).

Wind speed	Surface friction velocity	Surface average Langmuir turbulence number La_{sL}	Initial mixed layer depth
5	0.0055	0.61	20
6	0.0063	0.51	20
7	0.0077	0.48	20
8	0.0084	0.43	20
9	0.0095	0.43	20
10	0.0105	0.42	20
11	0.0122	0.44	20
12	0.0134	0.45	20
13	0.0151	0.47	20
5	0.0055	0.67	25
6	0.0063	0.56	25
7	0.0077	0.50	25
8	0.0084	0.43	25
9	0.0095	0.41	25
10	0.0105	0.40	25
11	0.0122	0.41	25
12	0.0134	0.42	25
13	0.0151	0.43	25
5	0.0055	0.73	30
6	0.0063	0.60	30
7	0.0077	0.54	30
8	0.0084	0.47	30
9	0.0095	0.43	30
10	0.0105	0.39	30
11	0.0122	0.40	30
12	0.0134	0.40	30
13	0.0151	0.41	30
5	0.0055	0.79	35
6	0.0063	0.65	35
7	0.0077	0.58	35
8	0.0084	0.50	35
9	0.0095	0.45	35
10	0.0105	0.42	35
11	0.0122	0.40	35
12	0.0134	0.39	35
13	0.0151	0.40	35

is based on the CVMix-KPP model (Large et al., 1994; Van Roekel and Coauthors, 2018), where the LT-induced eddy diffusivity is added to the CVMix-KPP model. In this paper, we modify Li et al. (2019)'s source code to replace it with our wave-induced parameterization. The experiments are conducted at 144.9° W and 50.1° N, which is near the Ocean Climate Station Papa (https://www.pmel.noaa.gov/OCS/Papa) in the northern Pacific. In the experiments, temperature and salinity are obtained from the Papa observatory, and the initial and forcing field data are from the wave rider buoy data recorded there (Belka et al., 2014), more data information can be found in Li et al. (2019). The GOTM5 time step is set to 1 min, and the results are output every 3 h. The total simulation time is 703.75 days, starting on January 1, 2012 and ending on December 4, 2013. There are 150 vertical levels with 1 m intervals, extending from the surface to 150 m. There are two sets of experiments: GOTM LB, which results from parameterization considering wave effects (both LT enhancement and BW), and GOTM no LB, which is the result of the parameterization without wave effects.

2.3. Statistical method

In Dong et al. (2011), mean square error (MSE), skill score (SS) and weighted skill score (WSS) are used. The mean square error (MSE) between the observation and model results is expressed as:

$$MSE_{i}(n) = \frac{1}{N_{i}} \sum_{j=1}^{N_{i}} (m_{i}(j, n) - o_{i}(j))^{2}$$
(5)

where the subscript i represents the variable (temperature and MLD); j

represents the observed data point, N_i is the number of observed data for variable i, n represents the experiment (GOTM LB and GOTM no LB), m_i and o_i represent the model and observed data, respectively.

Murphy (1992) proposed a skill score method based on a reference experiment (Equation (6)):

$$SS_i(n) = 1 - \frac{MSE_i(n)}{MSE_r} \tag{6}$$

where subscript r represents the reference experiment. When SS=0, there is no improvement compared to the reference experiment. When SS<0, the experiment has a lower performance relative to the reference experiment. When SS is between 0 and 1, there is an improvement compared to the reference experiment.

Since the numbers of available observation data for each variable is different, a weighted skill score (WSS) based on the number of observed values is used:

$$WSS(n) = 1 - \frac{WMSE(n)}{WMSE_r} \tag{7}$$

$$WMSE(n) = \frac{\sum_{i=1}^{I} (MSE_i(n)N_i)}{\sum_{i=1}^{I} N_i}$$
 (8)

where I is the total number of variables. The number of data points used were 5631 and 563 for temperature and MLD, respectively. Wilkin (2006) and Liu et al. (2009) both use this method.

3. The parameterization

In ocean and climate models, physical processes that cannot be solved directly are parameterized. Here we focus on the parameterization of vertical mixing within the OSBL. Usually, the mixing scheme applied to the upper ocean does not include BW and LT effects but instead focuses only on wind and convective forcing, such as the KPP scheme proposed by Large et al. (1994). Some recently proposed vertical mixing schemes that include the effect of LT are reviewed and compared in Li et al. (2019). But they do not consider the effect of BW. In this study, we propose a new mixing scheme based on the result of LES with the influence of LT and BW. The diffusivity $K_{\it diff}$ is diagnosed from LES using the equation $K_{diff} = -\overline{\theta w}/(\partial \Theta/\partial z)$, where θ is the temperature perturbation, w is the vertical velocity perturbation and Θ is the mean temperature. A non-dimensional parameter scaling method is used to analyze the eddy diffusivity. Surface friction velocity (u^*) and boundary layer depth (h_h) are used to scale and transform eddy diffusivity into a dimensionless variable $(K_{diff}/(u^*h_b))$. The remaining dimensional diffusivity no longer depends on depth after this function is derived. In this study, we define the boundary layer depth as the depth where the turbulent heat flux approaches zero. Eddy diffusivity below the boundary layer is affected by other processes that are not included in this study such as breaking internal waves. Here we focus on improving the mixing within the boundary layer.

After dimensionless processing, the effects of waves are directly calculated as follows:

$$K_d / (u^* h_{bK}) = K / (u^* h_{bK}) - K_\theta / (u^* h_{bK\theta})$$
 (9)

where K is the eddy diffusivity diagnosed from LES with wave influence, K_{θ} is the eddy diffusivity diagnosed from LES without wave influence and K_d is the wave-induced eddy diffusivity. h_{bK} and $h_{bK\theta}$ are the boundary layer depth of the corresponding experiment. Fig. 1 is the non-dimensional eddy diffusivity distribution for LES experiments. The red curve represents the non-dimensional eddy diffusivity $(K/(u^*h_{bK}))$ under different wind speeds, stratifications and surface average Langmuir numbers (Table 1) and the blue curve represents the corresponding non-dimensional eddy diffusivity $(K_{\theta}/(u^*h_{bK\theta}))$ without the wave influence. According to the form of eddy diffusivity (Large et al.,1994), We assume

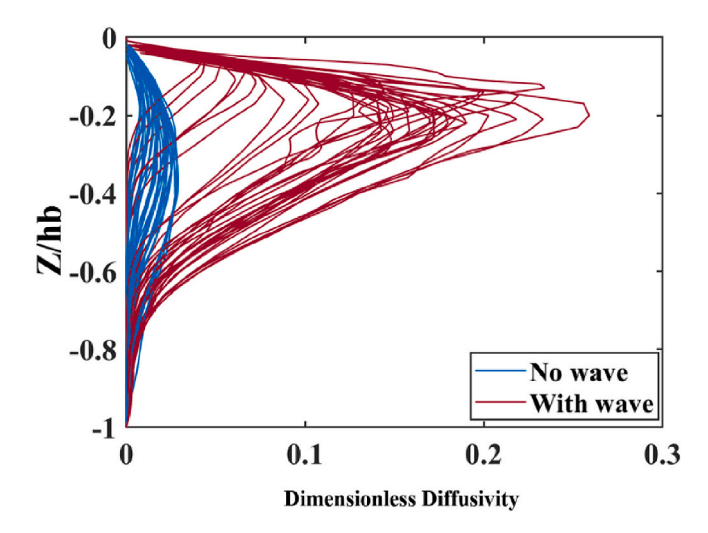


Fig. 1. Vertical distribution of eddy diffusivity curves. Red curves: experiments under different wind speeds, stratifications and surface average Langmuir numbers, K/u^*h_{bK} . Blue curves: the corresponding experiment without the wave effects, $K_\theta/u^*h_{bK\theta}$.

the wave-induced eddy diffusivity K_d has a form of $K_d = h_{bk}YG$. Y is the velocity scale. For simplicity, Y is set as u^* , since the variables of our sensitivity test are boundary layer depth and La_{sL} , the shape function (G) of the dimensionless eddy diffusivity is assumed to depend on the dimensionless depth $\sigma = z/h_b(0 \le |\sigma| \le 1)$ and La_{sL} , that is $G(\sigma, La_{sL})$, $G(\sigma, La_{sL}) = K_d/u^*h_{bk}$. With Equation (9):

$$G(\sigma, La_{sL}) = K / (u^* h_{bK}) - K_{\theta} / (u^* h_{bK\theta})$$

$$\tag{10}$$

By fitting the dimensionless curves (Equation (10)), the following functional relation is selected with parameters A and B:

$$K_d(\sigma, u^*, h_b, La_{sL}) / (u^*h_b) = G(\sigma, La_{SL}) = -\sigma \exp(-A(\sigma)^2 + B),$$

or

$$K_d\left(\frac{z}{h_b}, u^*, z, La_{sL}\right) = -u^* \times z \times \exp\left(-A\left(\frac{z}{h_b}\right)^2 + B\right)$$
(11)

Different fitting curves $(K/u^*h_{bK}-K_\theta/u^*h_{bK\theta})$ in Fig. 1 corresponds to different maximum curvature of the shape function G determined by parameters A and B. As the shape function $G(\sigma,La_{SL})$ is related to the surface average Langmuir number, Fig. 2a and b displays the relationship between A and B, and the average Langmuir number, respectively. As the parameterization is obtained under the experimental conditions is less than 1 (Table 1). The range of simulated Langmuir numbers corresponds predominately to values 0.2–0.5 reported for field measurements

(Smith, 1992). The wave-induced mixing parameterization is suitable for Langmuir turbulence numbers less than 1. A and B are expressed as functions depending on La_{sL} as follows:

$$A = 0.5 \exp\left(4\sqrt{La_{SL}}\right)$$

$$B = 6La_{SL} - 11\sqrt{La_{SL}} + 5$$
(12)

Our parameterization is different from other schemes. First, we use the wind speed to calculate the Stokes drift in our experiment setting for LES, which differs from other studies that use specified monochromatic waves (e.g. Noh et al., 2004). Also, BW is considered together with LT in the parameterization through the wind speed. Our parameterization differs from others in that it is KPP-based, unlike Harcourt (2015) or Reichl and Li (2019), our theory does not solve higher-order closures; it is closer to the similarity theories underpinning KPP and Monin-Obukhov, albeit with a different shape function than Troen and Mahrt (1986), who obtained their results from simple polynomials fitting of the atmospheric boundary layer formulations.

4. Test and discussion

4.1. Eddy diffusivity

GOTM5 can directly output the eddy diffusivity coefficient as it simulates an evolving parameterized boundary layer. Fig. 3 shows the vertical profile of eddy diffusivity for temperature at different times in the single-column simulation at Ocean Climate Station Papa. The eddy diffusivity increases from 0.0340 m²/s without wave-induced mixing (Fig. 3a, red line) to 0.1604 m²/s with wave-induced mixing (Fig. 3a, blue line). The corresponding surface friction velocity and surface average Langmuir turbulence number are 0.0115 m/s and 0.55. respectively. In Fig. 3b, the maximum eddy diffusivity is 0.0051 m²/s without the wave-induced mixing. By adding the wave-induced mixing, the eddy diffusivity coefficient increases to 0.0287 m²/s, roughly doubling the diffusivity. The corresponding surface friction velocity and Langmuir turbulence number are 0.0068 m/s and 0.53, respectively. Fig. 3c compares the maximum eddy diffusivity value from GOTM experiments GOTM LB and GOTM no LB. An annual cycle variation, starting in winter, is observed. When wave-induced mixing is considered in the parameterization scheme (GOTM LB), the maximum value can reach 0.9 m²/s in winter. The eddy diffusivity value is very small in summer and autumn, and the maximum eddy diffusivity changes with the season. Note that the addition of waves in all cases leads to stronger and deeper mixing.

4.2. Temperature and mixed layer depth

Direct comparison of the GOTM results with observation data (such as temperature, salinity and current velocity) may require additional external forcing beyond 1D mixing, such as horizontal and vertical

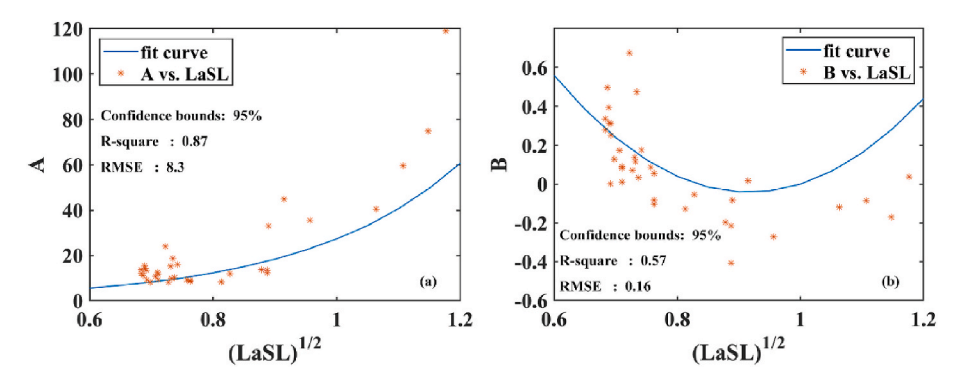


Fig. 2. Relationship between the surface average Langmuir number and (a) parameter *A*; and (b) parameter *B*. The orange dots and blue curve represent the data and fitting curves, respectively.

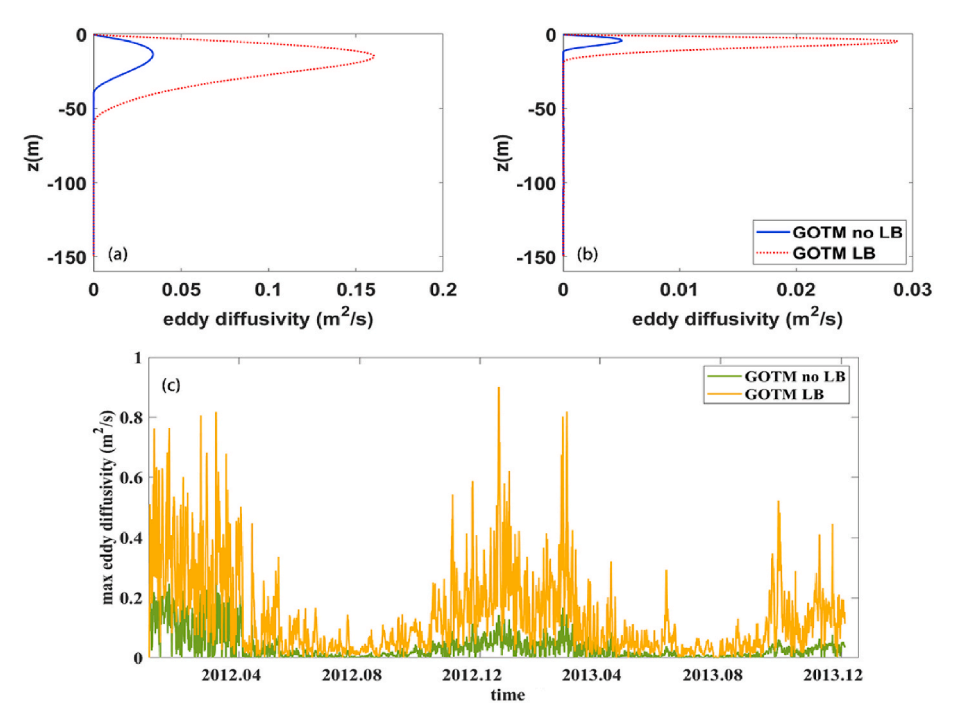


Fig. 3. Eddy diffusivity profiles of GOTM experiments. (a) 2012.11.12 06:00; (b) 2013.07.20 06:00. The red and blue curves are the eddy diffusivity distribution without and with wave-induced mixing, respectively. (c) Time series of the maximum eddy diffusivity value from GOTM results. The yellow and green curves are the results with and without wave-induced mixing, respectively.

advection, to adjust the heat and salt budget. Without these additional adjustments, the simulated variables (e.g. temperature and salinity) deviate from the observed values and lead to the imbalance of surface fluxes. Therefore, we compare the simulation and observations indirectly, that is, to verify if the LT and BW changes bring the result closer to the observations while noting that there are external forcing present that cannot be taken into account. The comparison aims to demonstrate the improvement of the results due to wave effects in the parameterization scheme.

Fig. 4 is the vertical profile of temperature at different times. Fig. 4a and b correspond to Fig. 3a and b, respectively. For simplicity, the mixed layer in Fig. 4 is where $|\text{T-T}_0|{>}0.5~\text{°C}$ is located. Fig. 4a shows that the MLD is 44.5 m and SST is 12.1 °C without wave-induced mixing. When the parameterization with wave effect is applied, the MLD is 62.5 m and the SST is 10.9 °C, which is closer to the observed MLD and SST of 63.5 m and 8.2 °C, respectively. Fig. 4 (b) shows that the MLD increases from 16.5 m (without wave-induced mixing) to 22.5 m (with wave-induced mixing). The corresponding SSTs are 18.9 °C and 16.2 °C, respectively. The observed MLD and SST are 24.5 m and 12.9 °C, respectively. Thus, applying the new parameterization with wave-induced mixing to a

realistic marine environment shows that the temperature and MLD tend to be closer to observations. The simulated temperature without wave influence is warmer than that with wave influence. Wave-driven mixing provides more mixing, bringing up deeper, denser water, thus improving the surface temperature match. The parameterization with wave influence thereby reduces this temperature bias. Comparing the observed MLD, the parameterization scheme without wave effect simulates a shallower mixed layer. The new parameterization scheme with wave effect deepens the MLD, again agreeing more closely with the observations. Therefore, the new parameterization scheme more accurately simulates temperature and MLD than the parameterization without wave effects in the GOTM experiments. For future research, the parameterization will be applied to a climate model to confirm the

Fig. 5 is the annual SST time series at Ocean Climate Station Papa (50° N, 145° W, https://www.pmel.noaa.gov/ocs/Papa). The GOTM-simulated temperature trend is consistent with the observed value, but there is a temperature deviation between the experiments with and without wave effects. The GOTM simulations cannot match the observations completely as other horizontal process influences (such as eddies

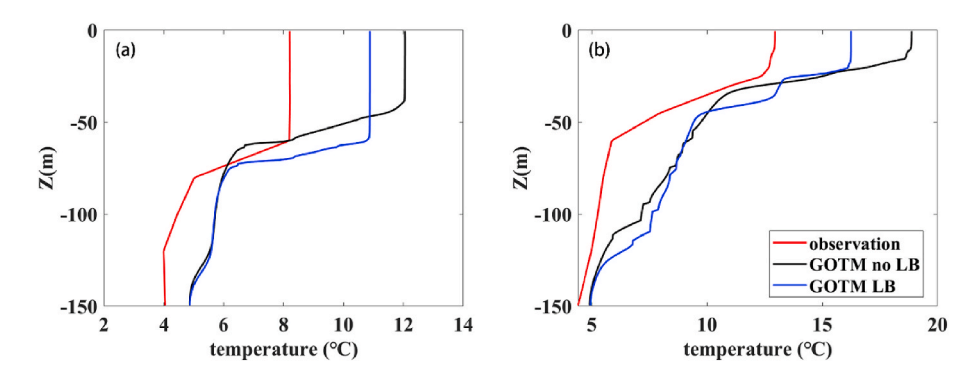


Fig. 4. Vertical temperature profile from GOTM, with time corresponding to Fig. 3. The blue curve represents the GOTM results with wave effects, the black curve represents the GOTM results without wave-induced mixing, and the red curve is the observation data.

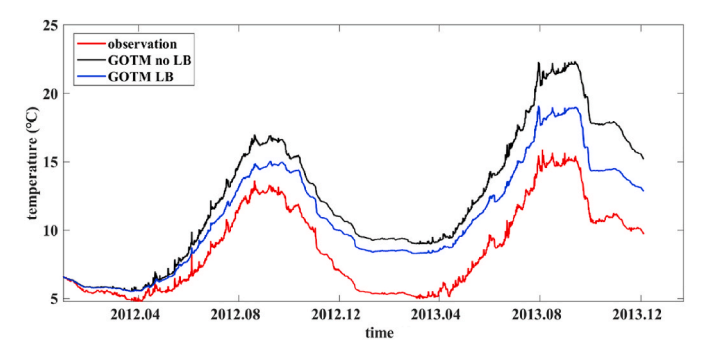


Fig. 5. Time series of temperature changes, starting from January 1, 2012. The blue and black curve represents the GOTM results with and without wave effects, respectively, and the red curve is the observation data.

and fronts). Furthermore, since errors tend to accumulate, any errors that affect the stratification early in the simulation also ripple to the results later in the simulation. Nonetheless, it should be noted that wave effects separating GOTM LB from GOTM no LB becomes more evident as temperature increases. The figure shows two peaks for temperature, both appearing in summer. The wave-induced mixing influence on temperature is strongest in summer and weakest in winter. Therefore, including the wave effects can reduce the overestimated SST in summer. Fig. 6 shows the time series of the MLD. The mixed layer is defined as the depth where the absolute difference between the temperature and the surface temperature is 0.5 °C. The difference between the simulated and observed values is smaller in spring and summer, which may be related to seasonal heat flux changes (Alford, 2020). Since this study focuses on improving parameterizations, no further analyses are made on the physical mechanism of shallower MLD in summer. However, when the wave effect is considered in the parameterization, the mixing layer obviously deepens in winter. Nevertheless, the effect is not particularly obvious in summer, which is consistent with the seasonality of waves in the North Pacific. Thus, this parameterization features a summertime SST cooling and a wintertime deepening of the mixed layer.

4.3. Statistical analysis

To quantify the experimental model results, we apply the statistical method mentioned in Dong et al. (2011) to temperature and MLD depth. The results are shown in Table 2. The MSE of temperature is 18.2 (7.1) when the parameterization without (with) wave effect is used. The MSE of the MLD is 648.7 (215.3) without (with) wave effects. Therefore, the parameterization with wave effects produces more accurate results than that without wave effects. The influence of SS on waves is evaluated with the GOTM no LB experiment as the reference. The SS_T of GOTM LB is 0.61 (according to Equation (6)), meaning that the GOTM LB temperature simulation has an improvement of 61% as compared to GOTM no LB. The SS_H of GOTM LB is 0.67, which means that the MLD simulation is improved by 67% relative to the GOTM no LB experiment. The weighted skill score analysis of the GOTM LB experiment is 0.66. That is, the simulation with the wave-induced mixing parameterization is 66% more accurate than the parameterization without wave effect. To sum up, the temperature and mixing layer depth simulation are improved by the parameterization scheme with wave effect, although including climatological upwelling would play a larger role than this wave-induced adjustment. The study conducted by Johnson et al. (2016) is an example of an alternative observational analysis intended to reduce this effect.

5. Conclusions

In the current study, a parametric equation of wave-induced mixing, including average surface Langmuir turbulence number, surface friction

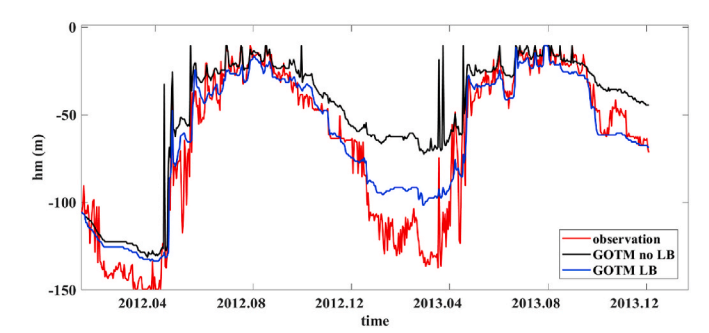


Fig. 6. Same as Fig, 5, but for mixed layer changes.

Table 2
MSE, SS and WSS of the GOTM LB and GOTM no LB experiments. T and H represent temperature and MLD, respectively.

EXP	MSE _T	SS_T	MSE_H	SS_H	WSS
GOTM no LB	18.2	0	648.7	0	0
GOTM LB	7.1	0.61	215.3	0.67	0.66

velocity, boundary layer depth and seawater depth, is obtained by analyzing LES model results. A new parameterization based on wave-induced eddy diffusivity is added to the KPP turbulence model. The new parameterization is then applied into the GOTM for verification, and the results from the experiments GOTM no LB (parameterization without wave effect) and GOTM LB (parameterization with wave effect) are compared.

It is found that the temperature trend from GOTM is consistent with the observed temperature. In summer, the effect of wave-induced mixing on temperature is higher than in winter. The wave-induced mixing can reduce the overestimated temperature in summer, but the influence on the MLD in summer is not particularly obvious and almost unchanged. However, it deepens the MLD in winter. Wave-induced mixing can improve temperature simulation in summer and reduce the underestimation of the MLD in winter.

Three statistical analyses are conducted, namely, MSE, SS and WSS. The parameterization scheme with wave effects is closer to the observed profile results than the parameterization scheme without wave effects. The parametric equation still requires further verification. Due to the limited conditions in the GOTM testing cases, the parametric equation will be added into a climate model for verification in future experiments, which allows for a broader range of conditions and the inclusion of effects such as climatological upwelling and lateral influences that are neglected here in this initial assessment of the parameterization.

Author statement

Haili Wang Experiment, Formal analysis, and Writing – Original Draft; Changming Dong Methodology and Writing – Review & Editing; Baylor Fox-Kemper Methodology and Writing – Review & Editing; Qing Li Analysis and Writing – Review & Editing; Yongzeng Yang Writing – Review & Editing; Xu Chen Writing – Review & Editing; Kenny T.C. Lim Kam Sian Writing – Review & Editing.

Declaration of competing interest

The authors declare that they have no known competing financial interests or personal relationships that could have appeared to influence the work reported in this paper.

Acknowledgements

This research was funded by the National Key Research and

Development Program of China (2017YFA0604100), NSF 1655221, the Natural Science Foundation of Jiangsu Province (Grants No. BK20170953), the National Natural Science Foundation of China (Grant No. 41706094, 42176023) and National Programme on Global Change and Air-Sea Interaction (Project No. GASI-IPOVAI-02). The authors are grateful to Yign Noh and appreciate the support of the China Scholarship Council (CSC).

References

- Alford, M.H., 2020. Revisiting near-inertial wind work: slab models, relative stress, and mixed layer deepening. J. Phys. Oceanogr. 50, 3141–3156. https://doi.org/ 10.1175/JPO-D-20-0105.1.
- Ali, A., Christensen, K.H., Breivik, Ø., Malila, M., Raj, R.P., Bertino, L., Chassignet, E.P., Bakhoday-Paskyabi, M., 2019. A comparison of Langmuir turbulence parameterizations and key wave effects in a numerical model of the North Atlantic and Arctic Oceans. Ocean Model. 137, 76–97. https://doi.org/10.1016/j. ocemod.2019.02.005.
- Balaguru, K., Foltz, G.R., Leung, L.R., Asaro, E.D., Emanuel, K.A., Liu, H., Zedler, S.E., 2015. Dynamic Potential Intensity: an improved representation of the ocean's impact on tropical cyclones. Geophys. Res. Lett. 42, 6739–6746. https://doi.org/ 10.1002/2015GL064822.
- Belcher, S.E., Grant, A.L.M., Hanley, K.E., Fox-Kemper, B., Van Roeke, L., Sullivan, P.P., Large, W.G., Brown, A., Hines, A., Calvert, D., Rutgersson, A., Pettersson, H., Bidlot, J.R., Janssen, P.A.E.M., Polton, J.A., 2012. A global perspective on Langmuir turbulence in the ocean surface boundary layer. Geophys. Res. Lett. 39, 1–9. https://doi.org/10.1029/2012GL052932.
- Belka, D.J., Schwendeman, M., Thomson, J., Cronin, M.F., 2014. Historical Wave and Wind Observations at Ocean Station, pp. 1–17.
- Cavaleri, L., Fox-Kemper, B., Hemer, M., 2012. Wind waves in the coupled climate system. Bull. Am. Meteorol. Soc. 93, 1651–1661. https://doi.org/10.1175/BAMS-D-11-00170.1.
- Craik, A.D.D., Leibovich, S., 1976. A rational model for Langmuir circulations. J. Fluid Mech. 73, 401–426. https://doi.org/10.1017/S0022112076001420.
- D'Asaro, E.A., Thomson, J., Shcherbina, A.Y., Harcourt, R.R., Cronin, M.F., Hemer, M.A., Fox-Kemper, B., 2014. Quantifying upper ocean turbulence driven by surface waves. Geophys. Res. Lett. 41, 102–107. https://doi.org/10.1002/2013GL058193.
- Dong, C., McWilliams, J.C., Hall, A., Hughes, M., 2011. Numerical simulation of a synoptic event in the Southern California Bight. J. Geophys. Res. Ocean. 116 https:// doi.org/10.1029/2010JC006578.
- Fan, Y., Griffies, S.M., 2014. Impacts of parameterized Langmuir turbulence and nonbreaking wave mixing in global climate simulations. J. Clim. 27, 4752–4775. https://doi.org/10.1175/JCLI-D-13-00583.1.
- Harcourt, R.R., 2015. An improved second-moment closure model of Langmuir turbulence. J. Phys. Oceanogr. 45, 84–103. https://doi.org/10.1175/JPO-D-14-
- Harcourt, R.R., 2013. A second-moment closure model of Langmuir turbulence. J. Phys. Oceanogr. 43, 673–697. https://doi.org/10.1175/JPO-D-12-0105.1.
- Harcourt, R.R., D'Asaro, E.A., 2008. Large-eddy simulation of Langmuir turbulence in pure wind seas. J. Phys. Oceanogr. 38, 1542–1562. https://doi.org/10.1175/ 2007JP03842.1.
- Johnson, L., Lee, C.M., D'Asaro, E.A., 2016. Global estimates of lateral springtime restratification. J. Phys. Oceanogr. 46, 1555–1573. https://doi.org/10.1175/JPO-D-15-0163.1.
- Kantha, L.H., Anne Clayson, C., 2004. On the effect of surface gravity waves on mixing in the oceanic mixed layer. Ocean Model. 6, 101–124. https://doi.org/10.1016/S1463-5003(02)00062-8
- Kenyon, K.E., 1969. Stokes drift for random gravity waves. J. Geophys. Res. 74, 6991–6994.
- Kukulka, T., Harcourt, R.R., 2017. Influence of Stokes drift decay scale on Langmuir turbulence. J. Phys. Oceanogr. 47, 1637–1656. https://doi.org/10.1175/JPO-D-16-0244.1.
- Lane, E.M., Restrepo, J.M., McWilliams, J.C., 2007. Wave–current interaction: a comparison of radiation-stress and vortex-force representations. J. Phys. Oceanogr. 37, 1122–1141. https://doi.org/10.1175/JPO3043.1.
- Large, W.G., McWilliams, J.C., Doney, S.C., 1994. Oceanic vertical mixing: a review and a model with a nonlocal boundary layer parameterization. Rev. Geophys. 32, 363–403. https://doi.org/10.1029/94RG01872.
- Large, W.G., Pond, S., 1982. Sensible and latent heat flux measurements over the ocean. J. Phys. Oceanogr. 12, 464–482. https://doi.org/10.1175/1520-0485(1982) 012<0464:SALHFM>2.0.CO;2.
- Li, Q., Fox-Kemper, B., 2017. Assessing the effects of Langmuir turbulence on the entrainment buoyancy flux in the ocean surface boundary layer. J. Phys. Oceanogr. 47, 2863–2886. https://doi.org/10.1175/JPO-D-17-0085.1.
- Li, Q., Reichl, B.G., Fox-Kemper, B., Adcroft, A.J., Belcher, S.E., Danabasoglu, G., Grant, A.L.M., Griffies, S.M., Hallberg, R., Hara, T., Harcourt, R.R., Kukulka, T., Large, W.G., McWilliams, J.C., Pearson, B., Sullivan, P.P., Van Roekel, L., Wang, P., Zheng, Z., 2019. Comparing ocean surface boundary vertical mixing schemes including Langmuir turbulence. J. Adv. Model. Earth Syst. 11, 3545–3592. https://doi.org/10.1029/2019MS001810.
- Li, Q., Webb, A., Fox-Kemper, B., Craig, A., Danabasoglu, G., Large, W.G., Vertenstein, M., 2016. Langmuir mixing effects on global climate: WAVEWATCH III

- in CESM. Ocean Model. 103, 145–160. https://doi.org/10.1016/j.ocemod.2015.07.020.
- Liu, Y., MacCready, P., Hickey, B.M., Dever, E.P., Kosro, P.M., Banas, N.S., 2009. Evaluation of a coastal ocean circulation model for the Columbia river plume in summer 2004. J. Geophys. Res. Ocean. 114, 1–23. https://doi.org/10.1029/ 2008.IC004929
- Maronga, B., Gryschka, M., Heinze, R., Hoffmann, F., Kanani-Sühring, F., Keck, M., Ketelsen, K., Letzel, M.O., Sühring, M., Raasch, S., 2015. The Parallelized Large-Eddy Simulation Model (PALM) version 4.0 for atmospheric and oceanic flows: model formulation, recent developments, and future perspectives. Geosci. Model Dev. (GMD) 8, 2515–2551. https://doi.org/10.5194/gmd-8-2515-2015.
- McWilliams, J.C., Restrepo, J.M., 1999. The wave-driven ocean circulation. J. Phys. Oceanogr. 29, 2523–2540. https://doi.org/10.1175/1520-0485(1999)029<2523: TWDOCs 2.0.CO:2.
- McWilliams, J.C., Restrepo, J.M., Lane, E.M., 2004. An asymptotic theory for the interaction of waves and currents in coastal waters. J. Fluid Mech. 511, 135–178. https://doi.org/10.1017/S0022112004009358.
- McWilliams, J.C., Sullivan, P.P., 2000. Vertical mixing by Langmuir circulations. Spill Sci. Technol. Bull. 6, 225–237. https://doi.org/10.1016/S1353-2561(01)00041-X.
- McWilliams, J.C., Sullivan, P.P., Moeng, C.H., 1997. Langmuir turbulence in the ocean. J. Fluid Mech. 334, 1–30. https://doi.org/10.1017/S0022112096004375.
- Murphy, A.H., 1992. Climatology, persistence, and their linear combination as standards of reference in skill scores. Weather Forecast. 7, 692–698. https://doi.org/10.1175/ 1520-0434(1992)007<0692:CPATLC>2.0.CO;2.
- Noh, Y., Min, H.S., Raasch, S., 2004. Large eddy simulation of the ocean mixed layer: the effects of wave breaking and Langmuir circulation. J. Phys. Oceanogr. 34, 720–735. https://doi.org/10.1175/1520-0485(2004)034<0720;LESOTO>2.0.CO;2.
- Noh, Y., Ok, H., Lee, E., Toyoda, T., Hirose, N., 2016. Parameterization of Langmuir circulation in the ocean mixed layer model using LES and its application to the OGCM. J. Phys. Oceanogr. 46, 57–78. https://doi.org/10.1175/JPO-D-14-0137.1.
- Pierson, W.J., Moskowitz, L., 1964. A proposed spectral form for fully developed wind seas based on the similarity theory of S. A. Kitaigorodskii. J. Geophys. Res. 69, 5181–5190. https://doi.org/10.1029/jz069i024p05181.
- Qiao, F., Song, Z., Bao, Y., Song, Y., Shu, Q., Huang, C., Zhao, W., 2013. Development and evaluation of an Earth System Model with surface gravity waves. J. Geophys. Res. Ocean. 118, 4514–4524. https://doi.org/10.1002/jgrc.20327.
- Qiao, F., Yuan, Y., Yang, Y., Zheng, Q., Xia, C., Ma, J., 2004. Wave-induced mixing in the upper ocean: distribution and application to a global ocean circulation model. Geophys. Res. Lett. 31, 2–5. https://doi.org/10.1029/2004GL019824.
- Reichl, B.G., Li, Q., 2019. A parameterization with a constrained potential energy conversion rate of vertical mixing due to Langmuir turbulence. J. Phys. Oceanogr. 49, 2935–2959. https://doi.org/10.1175/JPO-D-18-0258.1.
- Smith, J.A., 1992. Observed growth of Langmuir circulation. J. Geophys. Res. 97, 5651. https://doi.org/10.1029/91jc03118.
- Smyth, W.D., Skyllingstad, E.D., Crawford, G.B., Wijesekera, H., 2002. Nonlocal fluxes and Stokes drift effects in the K-profile parameterization. Ocean Dynam. 52, 104–115. https://doi.org/10.1007/s10236-002-0012-9.
- Sullivan, P.P., McWilliams, J.C., 2010. Dynamics of winds and currents coupled to surface waves. Annu. Rev. Fluid Mech. 42, 19–42. https://doi.org/10.1146/ annurev-fluid-121108-145541.
- Suzuki, N., Fox-Kemper, B., 2016. Understanding Stokes forces in the wave-averaged equations. J. Geophys. Res. Ocean. 121, 3579–3596. https://doi.org/10.1002/ 2015/10011566
- Teixeira, M.A.C., Belcher, S.E., 2002. On the distortion of turbulence by a progressive surface wave. J. Fluid Mech. 458, 229–267. https://doi.org/10.1017/ S0022112002007838
- Troen, I.B., Mahrt, L., 1986. A simple model of the atmospheric boundary layer; sensitivity to surface evaporation. Boundary-Layer Meteorol. 37, 129–148. https://doi.org/10.1007/BF00122760.
- Umlauf, L., Burchard, H., 2005. Second-order turbulence closure models for geophysical boundary layers. A review of recent work. Continent. Shelf Res. 25, 795–827. https://doi.org/10.1016/j.csr.2004.08.004.
- van den Bremer, T.S., Breivik, 2018. Stokes drift. Philos. Trans. R. Soc. A Math. Phys. Eng. Sci. 376 https://doi.org/10.1098/rsta.2017.0104.
- Van Roekel, L., Coauthors, 2018. The KPP boundary layer scheme for the ocean: revisiting its formulation and benchmarking one-dimensional simulations relative to LES. J. Adv. Model. Earth Syst. 10, 2647–2685. https://doi.org/10.1029/ 2018MS001336.
- Van Roekel, L.P., Fox-Kemper, B., Sullivan, P.P., Hamlington, P.E., Haney, S.R., 2012. The form and orientation of Langmuir cells for misaligned winds and waves. J. Geophys. Res. Ocean. 117, 1–22. https://doi.org/10.1029/2011JC007516.
- Wang, H., Dong, C., Yang, Y., Gao, X., 2020. Parameterization of wave-induced mixing using the large eddy simulation (LES) (I). Atmosphere 11, 207. https://doi.org/ 10.3390/atmos11020207.
- Webb, A., Fox-Kemper, B., 2015. Impacts of wave spreading and multidirectional waves on estimating Stokes drift. Ocean Model. 96, 49–64. https://doi.org/10.1016/j. ocemod.2014.12.007.
- Webb, A., Fox-Kemper, B., 2011. Wave spectral moments and Stokes drift estimation. Ocean Model. 40, 273–288. https://doi.org/10.1016/j.ocemod.2011.08.007.
- Wilkin, J.L., 2006. The summertime heat budget and circulation of southeast New England shelf waters. J. Phys. Oceanogr. 36, 1997–2011. https://doi.org/10.1175/JPO.2968.1